

# The Physiological Characteristics and Related Genes of A Physiologically Etiolated Cabernet Sauvignon Grapevine\*

Chen Yingchun<sup>1,2</sup>, Du Yuanpeng<sup>1</sup>, Ji Xinglong<sup>1</sup>, and Zhai Heng<sup>1\*</sup>

1. College of Horticulture Science and Engineering, Shandong Agricultural University, State Key Laboratory of Crop Biology, Tai'an, Shandong 271018, China;

2. Shan-dong Academy of Grape, Jinan, Shandong 250100, China

**Abstract:** Physiologically etiolated Cabernet Sauvignon grapevine provide materials for the study of the structure and function of the photosynthetic system and gene expression and regulatory mechanisms. This study describes the analysis of an etiolated grapevine (*Vitis vinifera* L.cv. Cabernet Sauvignon). The leaves are light yellow, thin, and fragile, and the plants have smaller fruit clusters, with fruits that are lighter in both weight and color, than those of wild-type. The contents of chlorophyll a, chlorophyll b, and carotenoid were found to be significantly lower in etiolated leaves than in green leaves, while the etiolated leaves cells displayed structural defects, and the photosynthetic performance of the leaves was markedly reduced. Affymetrix GeneChip oligonucleotide arrays were employed to identify differentially expressed genes between the etiolated and control samples. A total of 2,911 and 775 genes displayed altered expression in the leaves and fruits, respectively, and were associated with various metabolic pathways. In particular, there was a significant repression of genes associated with photosynthesis, including the metabolism of porphyrin and chlorophyll, as well as genes involved in the synthesis of plant hormones and proteins. By contrast, there was significant upregulation of *AAT* genes, which are related to carbon fixation in photosynthetic organisms, *BZ1*, which is involved in anthocyanin biosynthesis, and *PaO* and *RCCR*, which function in chlorophyll degradation.

**Key words:** physiologically etiolated grapevine, microarray analysis, physiological response

## 1. Introduction

Physiologically etiolated Cabernet Sauvignon grapevine are ideal for the study of the structure and function of the photosynthetic system, the chlorophyll biosynthesis pathway, the development and regulatory mechanisms of chlorophyll. The economically important genus *Vitis*, with an available full genome

sequence, has become an ideal woody species for genomic studies. The grapevine (*Vitis vinifera* L.) is attractive for genomic research because it is diploid and has a small genome size (475 to 500 Mb) relative to that of other plants; the genome is approximately four times the size of the *Arabidopsis* genome and one sixth the size of the corn genome [1, 2], and it comprises 19 chromosomes. The genotypes of grape varieties are highly heterozygous, nearly all modern cultivated varieties (cultivars) are hermaphroditic and self-fertile, and they outcross easily. Over the past ten years, there has been a rapid increase in genomic resources available for grapevine research.

The French-Italian Public Consortium for Grapevine Genome Characterization published the draft sequence

\* This work was supported by a grant from the China Agriculture Research System (CARS-30). We are grateful for discussions and insightful input from Hao Yujin and Yao Yuxin.

Chen Yingchun and Du Yuan-Peng contributed equally to the article

**Corresponding author:** Zhai Heng, Professor, research area/interests: grapevine cultivation physiology. E-mail: hengz@sdau.edu.cn.

of the grapevine genome in *Nature* on 26 August 2007. This draft sequence represents the fourth such sequence produced for flowering plants thus far, the second for a woody species, and the first for a fruit crop (cultivated for both fruits and beverages). Affymetrix (<http://www.affymetrix.com/index.affx>) has released a grape array that represents 14,000 *V. vinifera* transcripts and 1,700 transcripts from other *Vitis* species, which will be useful for gene expression analysis. A 1,456,270-mer oligo set for investigating gene expression in grapevine is available from Qiagen (<http://www.qiagen.com>).

Terrier (2005) [3] used 50-mer oligoarrays bearing a set of 3,200 unigenes from *Vitis vinifera* to compare berry transcriptomes at nine developmental stages. Analysis of transcript profiles revealed that most activations were triggered simultaneously with softening, occurring within only 24 h for an individual berry, just before any change in coloration or water, sugar, or acid content could be detected. Fernandez (2006) [4] analyzed the *fleshless berry* mutant (*Vitis vinifera* L. cv Ugni Blanc), with dramatically reduced fruit size due to a lack of pericarp development, using oligo-specific arrays. Fifty-three and 50 genes were identified as being down- and upregulated, respectively, in this mutant. Giorgia (2009) [5] was the first to use Affymetrix GeneChip oligonucleotide arrays to identify differentially expressed genes between infected and recovered samples from Chardonnay and between infected and healthy samples from Manzoni Bianco. The authors found that 69 to 74% of the genes were expressed in the testing stage. The expression levels of 765 genes were found to be significantly altered, including some upregulated and some down-regulated genes. This study laid the foundation for utilizing the grape array.

In the current study, we describe the analysis of an etiolated Cabernet Sauvignon grapevine. Affymetrix GeneChip oligonucleotide arrays were employed to identify differentially expressed genes between the etiolated grapevine and control samples.

## 2. Materials and Methods

### 2.1 Plant Material

The physiologically etiolated Cabernet Sauvignon grapevine was discovered in the Yantai Great Wall vineyard of COFCO (China Oil & Foodstuffs Corporation) in 2008 (Fig. 1). The grapevine was planted in 2005 and was maintained on two sides of a trellage. The etiolated region of the Cabernet Sauvignon grapevine was in one arm of the vine, which had eight branches containing albino leaves and fruits, while the other side of the vine was normal. A Cabernet Sauvignon grapevine growing adjacent to the etiolated grapevine, with the same tree vigor and growing environment, was chosen as the control. The study was completed in Penglai in the COFCO vineyard in 2008 and 2009. In 2010, the grapevine was transplanted into a vat and brought to Shandong Agricultural University in Tai'an for further analysis.

### 2.2 Anatomical Analysis

Mature etiolated and control leaves were collected from a field in June, 2009. The leaves of the grape were cut into small blocks (1 mm × 2 mm), and double fixation was performed using 3.5% glutaraldehyde containing 0.1 mol/L phosphonic acid buffer (pH 7.3) and 1% osmic acid. These materials were dehydrated using an ethanol series and were then embedded in Epon 812. Specimens were sliced using an LKB-V microtome (LKB, Uppsala, Sweden), and the chloroplast structure of young leaves was observed using a JEOL-1200EX transmission electron microscope (JEOL, Tokyo, Japan).

### 2.3 Physiological Measurements

Photosynthetic data were collected from fully expanded leaves from 9:00 to 11:00 am on sunny days using an LI-6400 portable photosynthesis system. The etiolated side of the Cabernet Sauvignon grapevine was compared with the green side of the vine and the normal green control grapevine. The levels of Chl<sub>a</sub>,

Chlb, and Carotenoids on the same nodes of mature leaves and young leaves from the etiolated side of the Cabernet Sauvignon grapevine were monitored using the assay method of Lichtenthaler (1987) [6]. Grape clusters were picked from the etiolated branches and the controls. Experiments on etiolated fruit content were performed using conventional methods. The levels of soluble protein, soluble solids, and anthocyanin were all tested using an ultraviolet spectrophotometer. Photosynthetic parameters were measured using leaves from the fifth nodes of leaves with a pulse-modulated fluorometer (FMS-2,

Hansatech, UK). The maximum quantum efficiency of PSII primary photochemistry ( $F_v/F_m$ ) and dark respiration was determined after 30 min of dark adaptation. The maximum fluorescence ( $F_m$ ) yield was recorded during the application of a 0.8 s saturation flash ( $> 8,000 \text{ mmol m}^{-2} \cdot \text{s}^{-1}$ ). The maximum quantum efficiency of PSII primary photochemistry was calculated as  $(F_v/F_m) = (F_m - F_o)/F_m$ ,  $qP = (F_m' - F_s)/(F_m' - F_o')$ ,  $qN = (F_m - F_m')/(F_m - F_o')$ . Data were analyzed using the SPSS 13.0 statistical software package, and means were compared using a Duncan test ( $P < 0.05$ ).



**Fig. 1 Etiolated Cabernet Sauvignon Grapevine**

(A: Cabernet Sauvignon grapevine in Yantai Great Wall vineyard of COFCO; B: etiolated branches of Cabernet Sauvignon grapevine; C: the inflection point of the etiolated grapevine; D: comparison of etiolated fruit with control fruit)

#### 2.4 RNA Isolation

Total RNA was extracted from mature etiolated and control mature leaves and from fruits that were finely ground in liquid nitrogen using Qiagen RNeasy Plant MidiKit columns according to the manufacturer's instructions. The RNA samples were purified using a Qiagen RNeasy Kit, and an Agilent 2100 bioanalyzer was used to monitor sample quality.

#### 2.5 Microarray Hybridization

Affymetrix microarray hybridization was carried out by the Shanghai Bio Corporation. RNA target preparation and microarray hybridization were performed using a GeneChip 3' IVT Express Kit (Affymetrix) and GeneChip hybridization. A Wash and Stain Kit (Affymetrix) was employed following manufacturer's instructions. The signal intensity for

each probe set on the GeneChip microarray was detected with a GeneChip Scanner 3000 (Affymetrix), and the raw signal value for each probeset was analyzed with GeneChip Operating Software (GCOS; Affymetrix). Normalization of all arrays was performed by quantile normalization using MAS 5.0 to standardize the distribution of probe intensities for each array in a set of arrays.

### 2.6 Microarray Data Analysis

In this study, the filtered data were analyzed by two-way ANOVA given the effects of genotype and development stage using an R-package (The R Project for Statistical Computing, <http://www.r-project.org/>). The criteria of  $P < 0.01$ , used in combination with a fold change  $\geq 2$ , were selected for FDR (false discovery rate) processing to determine the final significantly differentially expressed (increased or decreased) transcripts. Annotations of probe sets were made using the publicly available NetAffx™ Analysis Center Website (NetAffx, <http://www.affymetrix.com/analysis/index.affx>).

The resulting differentially expressed genes that passed the conditions for filtration ( $P < 0.01$  and fold change  $\geq 2$ ) were subjected to principal component analysis (PCA) to obtain an overview of the transcriptome data. PCA is an unsupervised projection method used to extract systematic trends from large data sets where the number of variables is much larger than the number of objects. Hierarchical clustering analysis (HCA) is one of the most frequently used clustering approaches to untangle prominent expression patterns of array data. HCA was conducted using the Euclidean distance metric and average linkage for determining distance in the hierarchical tree. The resulting data were clustered and visualized using Cluster 3.0 and Treeview 1.1.0 software (<http://bonsai.hgc.jp/~mdehoon/software/cluster/software.htm>).

The functional annotations and categories of genes were based on Gene Ontology. Because there is a lack

of elaborate genome annotation for *Vitis*, biological functions of *Vitis* genes were made according to the closest *Arabidopsis* ortholog when necessary. *Vitis* sequences homologous to *Arabidopsis* were identified from the annotation on JGI. Ontological assignments available in TAIR, JGI, and the GO database [7] were used.

### 2.7 Quantitative Real-time PCR Validation of Expression Profiles

Samples used for qRT-PCR represented additional biological replicates from the same field sampling as those used in the microarray study, and independent RNAs were prepared for quantitative RT-PCR analysis. RNA extraction and quality control were performed as described above. cDNA was synthesized from 2  $\mu\text{g}$  of total RNA using Super-ScriptII (Invitrogen) with Oligo (dT) primers (Invitrogen) in a total volume of 25  $\mu\text{l}$  following the manufacturer's instructions. The reverse transcription mix was then diluted to a final volume of 50  $\mu\text{l}$ , and 1  $\mu\text{l}$  was used for the qRT-PCR experiments. Reactions were carried out using a StepOnePlus™ Real-Time PCR System (Applied Biosystems) with Power SYBR-Green PCR Master Mix (Applied Biosystems) and gene-specific primers. Cycling conditions were: initial denaturation (95°C, 10 min) followed by 40 cycles of denaturation (95°C, 15 s), annealing, and extension (60°C, 1 min). Candidate genes were tested in triplicate wells and in three duplicate experiments. The relative value for expression level of each gene was calculated by the  $2^{-\Delta\Delta\text{CT}}$  method using the poplar actin gene as an internal control [8].

## 3. Results

### 3.1 Physiological Characteristics of the Etiolated Grapevine

#### 3.1.1 Chlorophyll Content

The leaves of the etiolated grapevine Cabernet Sauvignon grapevine were light yellow, thin, and fragile. To ascertain the pigment content of the

etiolated grapevine, the pigment content was repeatedly assessed over a 3-year period. The contents of chlorophyll a, chlorophyll b, and carotenoid were significantly lower than those of green leaves, with mature leaf levels of only 1.27%, 1.10%, and 7.55% of wild-type level, respectively. In addition, the pigment contents of mature leaves were lower than those of young leaves (Table 1). A similar trend was observed with SPAD values (Soil and Plant Analyzer Development).

### 3.1.2 Physiological Changes in Etiolated Grapevine Fruits

The fruits of the etiolated Cabernet Sauvignon had smaller fruit clusters that were lighter in weight than those of the control (Fig. 2A). Because the seeds did not ripen well, the seeds failed to germinate in each of two years of planting. The contents of soluble solids, sugars, and soluble proteins were lower than those in the control, with only 66.67%, 60.67%, and 47.14% of control levels, respectively (Fig. 2B and D). The titrable acidity was 1.92-fold that of the control (Fig. 2B). The fruits of the etiolated Cabernet Sauvignon were light in color. In addition, the fruits had a greatly reduced anthocyanin content, with a level of only 56.44% compared with that of the control (Fig. 2C).

**Table 1 Pigment Content of Cabernet Sauvignon Etiolated Grapevine Leaves**

		Chla mg/g	Chlb mg/g	Chla + Chlb mg/g	Chla/Chlb	Cx.c mg/g
Young leaf	etiolated leaves	0.047c	0.022c	0.069c	2.114a	0.039c
	green leaves	2.473a	1.287a	3.761a	1.921b	0.275a
	CK	1.167b	0.629b	1.796b	1.856b	0.167b
Mature leaf	albino leaves	0.037c	0.017c	0.055c	2.138a	0.021c
	green leaves	2.895a	1.546a	4.442a	1.873b	0.278a
	CK	1.864b	0.923b	2.787b	2.020ab	0.220b

The data in the column followed by different small letters show significant difference at the 0.05 level (by Duncan test).

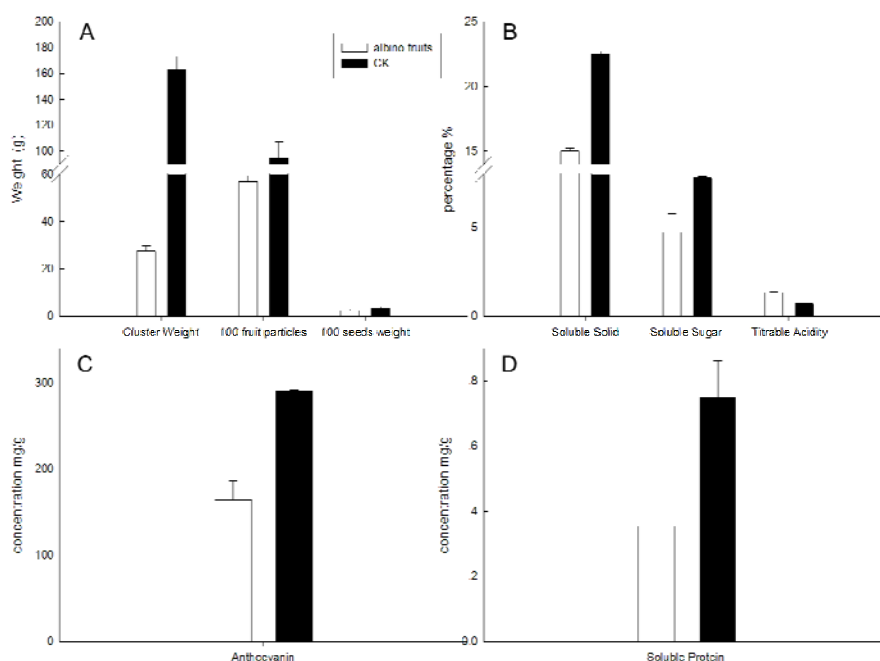


**Fig. 2 Distinctiveness of Etiolated Grapevine Fruits**

A: Cluster weight, 100 fruit particles, 100 seeds weight of albino fruits; B: Soluble solid, soluble sugar, titrable acidity of etiolated grapevine fruits; C: Anthocyanin of etiolated grapevine fruits; D: Soluble protein of etiolated grapevine fruits.

### 3.1.3 Photosynthetic Parameters

The level of photosynthesis of etiolated leaves was quite reduced, with a photosynthetic rate (Pn), Water Use Efficiency (WUE), and transpiration rate (Tr) all lower than those of two green controls (Fig. 3). In May of 2009, the Pn and Tr were only 13.12% and 18.28% of green branch levels, respectively, while the WUE was 72.48% that of the green branches. This may have resulted from the lower chlorophyll and water content in the etiolated leaves. The edges of the lower leaves in the albino branches began to dry out and senesce very early due to the serious deficiency

of photosynthetic product. In July of 2009, the Pn and WUE were only 3.66% and 8.24% of green branch levels, respectively, while Tr increased to 43.22% of green branch levels. By August, 2009, all of the etiolated leaves had already dropped off the grapevine. In May, 2010, the Pn, WUE and Tr were only 5.11%, 5.59%, and 75.39% of green branch values, respectively, indicating that the etiolated grapevine would subsequently become a weak grower. The green region of the etiolated grapevine plant showed no significant differences from the control for each of the photosynthesis-related parameters tested.

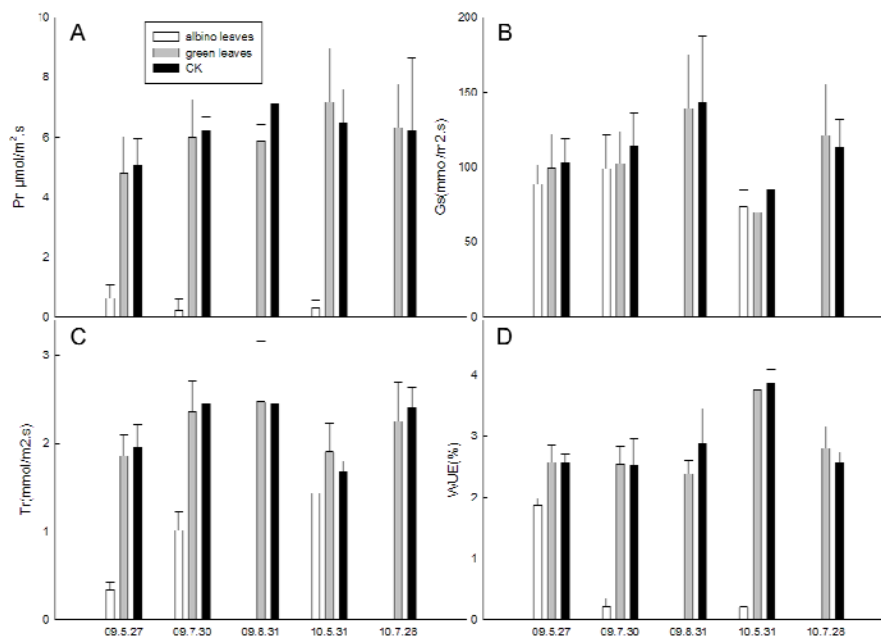


**Fig. 3 Comparison of Photosynthetic Parameters**

A: Pn of mature etiolated leaves; B: Gs of mature etiolated leaves; C: Tr of mature etiolated leaves; D: WUE of mature etiolated leaves. X-axis indicates different testing times, all of which occurred in August of 2010, when the etiolated leaves fell off the vines.

### 3.1.4 Chlorophyll Fluorescence Parameters in Etiolated Leaves

Chlorophyll fluorescence parameters were examined, including minimum fluorescence of dark adaptation (Fo), maximum fluorescence of dark adaptation (Fm), variable fluorescence (Fv), maximal photochemical efficiency of PSII (Fv/Fm), actual photochemical efficiency of PSII ( $\Phi\text{PSII}$ ), photochemical quenching coefficient (qP), non-photochemical quenching coefficient (NPQ), and the electron transfer rate (ETR)

(Fig. 4). The results showed that in the etiolated leaves, Fo, Fm, Fv, Fv/Fm,  $\Phi\text{PSII}$ , ETR, and qP levels were all decreased, while NPQ increased, but only in the July, 2009 test. The values for the green region of the etiolated grapevine were not significantly different from those of the control, except for the NPQ level tested in May, 2009.

## 3.2 Anatomical Structural Changes

### 3.2.1 Ultrastructural Variation of Chloroplasts

Chloroplasts are the sites of photosynthesis and the fixation of atmospheric carbon dioxide in green plant cells. The etiolated leaves cells exhibited structural defects. The levels of intracellular insoluble substances in etiolated leaves were slightly decreased, while the numbers of chloroplast in etiolated leaves vs. control leaves were approximately  $4.62 \pm 2.20$  and  $12 \pm 1.22$ , respectively. The chloroplast shape was significantly altered in the etiolated grapevine, and chloroplast aggregation was also observed. In general, two types of chloroplasts were detected, i.e., relatively flat, short chloroplasts with a square shape and flower-shaped vesicles (Fig. 5B and E), and slender chloroplasts (Fig. 5C and F). The control leaves had typically shaped

chloroplasts, with completely formed grana, stroma, thylakoids, and starch grains (Fig. 5A and D).

### 3.2.2 Ultrastructural Variation of Nuclei and Membranes

The nuclei in the cells of etiolated leaves has an irregular shape, with partially dissolved nuclear membrane (Fig. 6B), while the control nuclei were oval, with distinct edges (Fig. 6A). The cell membranes of etiolated leaves were incomplete, and the chloroplast and mitochondrial membranes were partially dissolved (Fig. 6D); however, no granulosus virus particles or exogenous pathogens were observed in the etiolated grapevine (Fig. 6C).

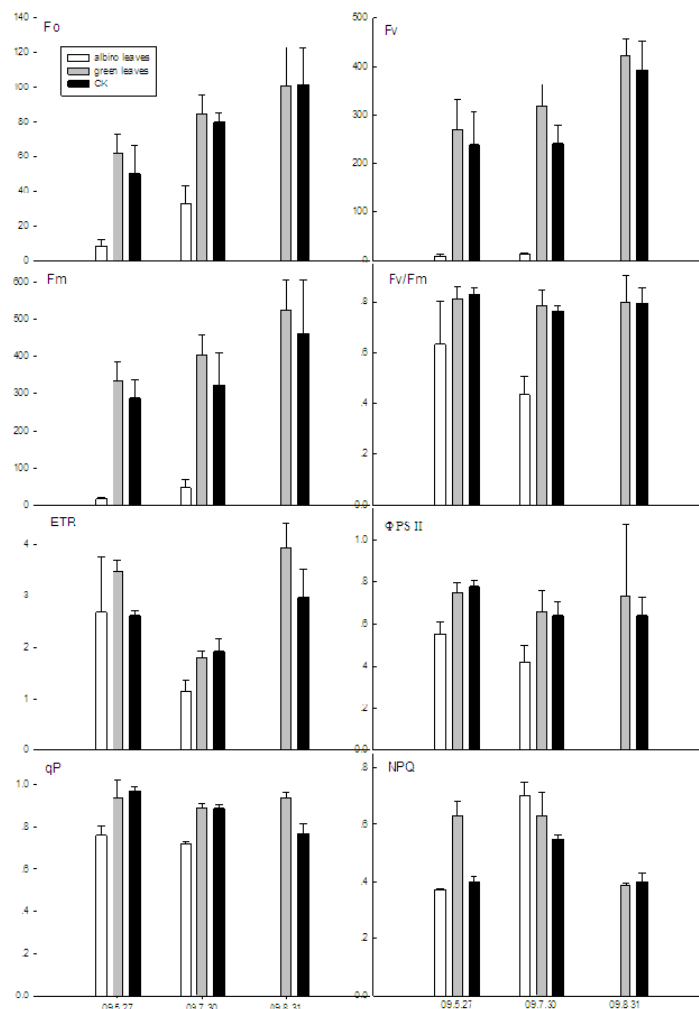


**Fig. 4 Chlorophyll Fluorescence Parameters in Etiolated Leaves**

Note: Comparison F<sub>0</sub>, F<sub>m</sub>, F<sub>v</sub>, F<sub>v</sub>/F<sub>m</sub>, ΦPS II, ETR, qP and NPQ of etiolated leaves with two green samples. X-axis means three different testing times.

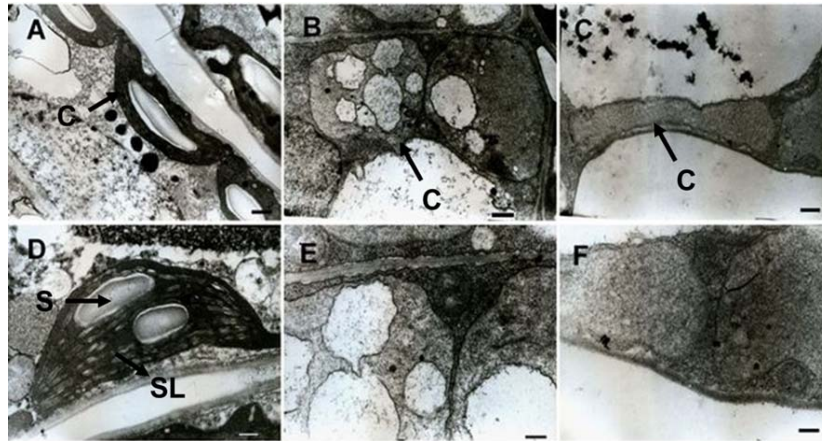


**Fig. 5 Comparison of the Ultrastructures of Etiolated and Control Leaves**

A, D: Ultrastructure of control leaf; B, E, C, F: Ultrastructure of etiolated leaf. C: Chloroplast; S: Starch grain; SL: Stromalamella. A, B, C: scale bars = 500 nm; D, E, F: scale bars = 200 nm.

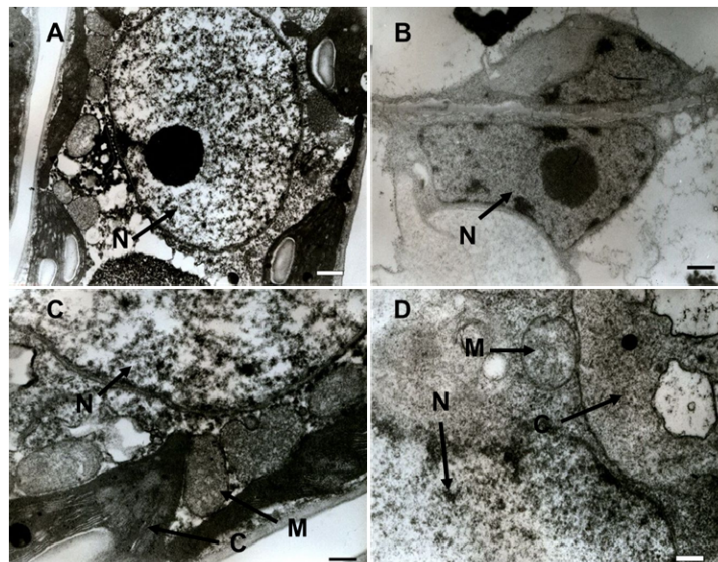


**Fig. 6 Comparison of Nuclei and Cell Membranes of Etiolated and Control Leaves**

A: Nucleus of control leaf cell; B: nucleus of etiolated leaf cell; C: membrane of etiolated leaf cell; D: membrane of control leaf cell. C: chloroplast; N: nucleolus; M: mitochondria. A, B: scale bars = 200 nm; C, D: scale bars = 500 nm

### 3.3 Global Gene Expression Profiles of Etiolated Leaves and Fruits

The economically important genus *Vitis*, with its available full genome sequence, has become an ideal woody species for genomic studies. The GeneChip *V. vinifera* genome array (Affymetrix) contains a large and significant portion of the 30,344 genes predicted for *V. vinifera* [9]. The GeneChip contains 16,436 probesets, including 14,496 derived from *V. vinifera* transcripts and 1,940 derived from other *Vitis* species

or hybrid transcripts. Sequences used in the design of the *Vitis* GeneChip were selected from GenBank, dbEST, and NCBI Reference Sequences (RefSeq).

A heat map of the most significantly differentially expressed genes (false discovery rate  $\leq 0.01$ ) from etiolated vs. control samples was constructed. Genes with similar expression patterns were grouped together. In this heat map, the color scale ranges from saturated green for log ratios of 2.0 and below (repression) to saturated red for log ratios of 2.0 and above (induction), whereas black indicates no change in transcript level.

## The Physiological Characteristics and Related Genes of A Physiologically Etiolated Cabernet Sauvignon Grapevine

Each gene is represented by a single row of colored boxes, and each experiment is represented by a single column.

Across the six arrays, approximately 16,603 genes were expressed at detectable levels in the leaf tissues. ANOVA with Benjamini-Hochberg (BH) adjustment of the false discovery rate (FDR) identified 2,911 probesets with  $FDR \leq 0.01$ , based on differences

between the etiolated grapevine and the control samples. As illustrated in Fig. 7, of the 2,911 probesets in the etiolated leaves, 1,261 genes were upregulated and 1,650 genes were downregulated (Fig. 7A), while in the albino fruit, 775 genes were detected, of which 397 were upregulated and 378 were downregulated (Fig. 7B). Additionally, the two tissues shared 184 probesets.

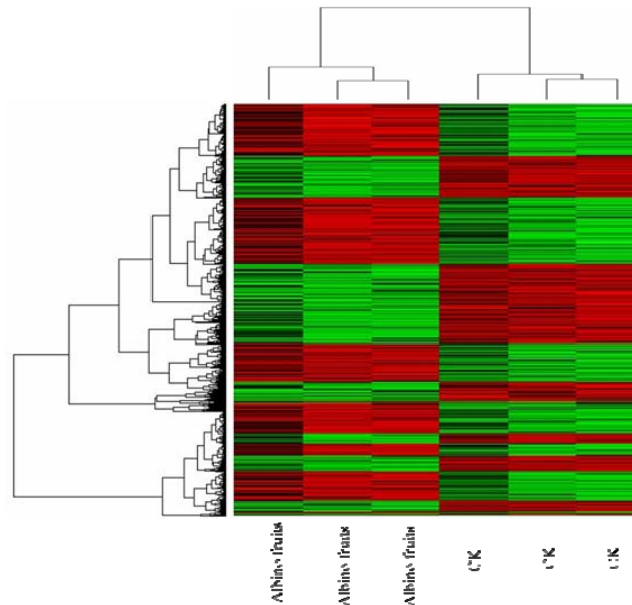


**Fig. 7A Heat Map Visualization of the 2,911 Most Significantly Differentially Expressed Genes in Etiolated Leaves Compared to Control Leaves**

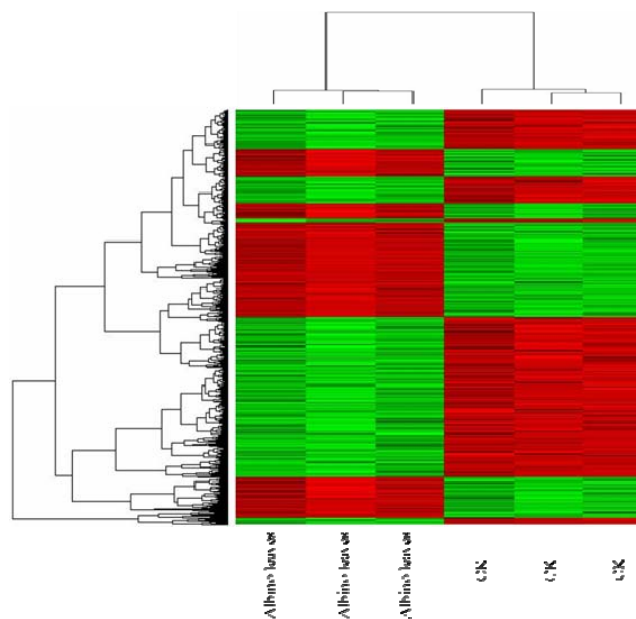


**Fig. 7B Heat Map Visualization of the 775 Most Significantly Differentially Expressed Genes in Etiolated Fruits Compared to Control Fruits**

### 3.4 Differentially Expressed Transcription Factors

Extracting information on the biological functions of differently regulated genes from array data is a major aspect of analysis. We categorized up- or downregulated genes into two genotypes according to Gene Ontology (GO) classifications [10]. Among the differently regulated array elements, we found that 2,911 genes corresponded to 306 functional categories. According to GO biological processes, 2,196 differently expressed genes were identified from albino leaf array data, covering 72.0% of all altered genes (Fig. 8A). As indicated, an overwhelming proportion of these genes were found to be associated with cellular process, metabolic process, biological regulation, response to stimulus, anatomical structure formation, and other functions.

Based on GO biological processes, 579 genes were identified from the etiolated fruit array data. Compared with leaves, the fruits lacked differently expressed genes involved in the positive regulation of biological or rhythmic processes (Fig. 8B). Genes with over two-fold increased expression levels in the etiolated grapevine were selected for further analysis ( $FDR \leq$

0.01). In etiolated leaves, genes with photosynthesis-related functions were repressed (Table 2). The *psaD* gene, which functions in the photosystem I reaction center subunit II, was the only gene with significantly downregulated expression, with a 5.04-fold decrease in expression, while the expression levels of other genes were outside the over two-fold range. In etiolated leaves, carbon fixation in photosynthetic organisms was also strongly affected. The genes that were upregulated in this pathway included pyruvate orthophosphate dikinase (PPDK), aspartate aminotransferase, and PCK1/PEPCK (phosphoenolpyruvate carboxykinase1). Among these, a spartate aminotransferase was significantly upregulated, with levels of approximately 24.56-fold those of the control. In plants, porphyrin and chlorophyll synthesis lead to increased levels of photosynthesis. However, the only significantly upregulated gene related to chlorophyll catabolism was the gene encoding pheophorbide a oxygenase. For flavonoid biosynthesis, three genes were inhibited, including genes encoding dihydroflavonol reductase, leucoanthocyanidin reductase 2, and innamate-4-hydroxylase.

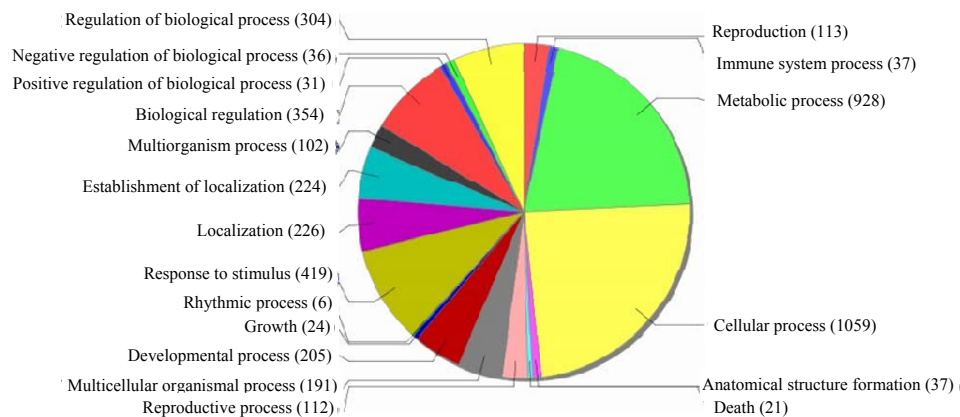


**Fig. 8A Functional Classification of Differentially Expressed Genes in Etiolated Leaves, Functional Categories Were Based on Biological Processes from GO Annotation**

### The Physiological Characteristics and Related Genes of A Physiologically Etiolated Cabernet Sauvignon Grapevine

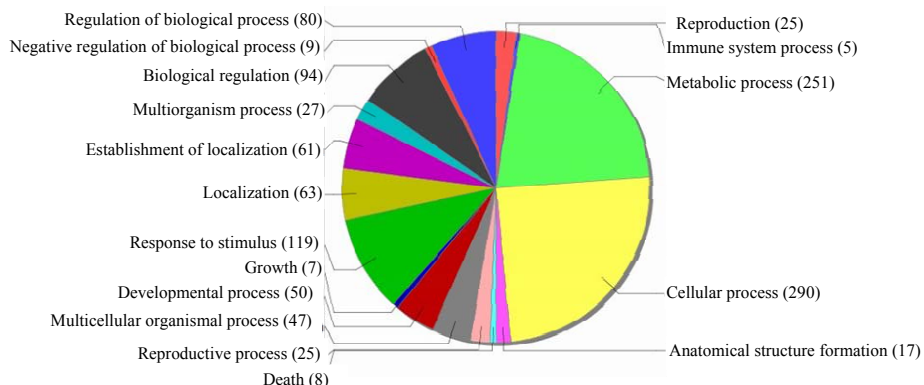


**Fig. 8B Functional Classification of Differentially Expressed Genes in Etiolated Fruits, Functional Categories Are Based on Biological Processes from GO Annotation.**

**Table 2 Induced Genes in Etiolated Leaves**

Probe ID	Description	Regulation	Fold change
Photosynthesis			
1611623_at	photosystem I reaction center subunit II	down	5.04
Carbon fixation in photosynthetic organisms			
1618753_at	pyruvate kinase	down	2.49
1620654_at	Hyponasticleaves 1 protein coding	down	3.42
1612414_at	Pyruvate orthophosphate dikinase PPK	up	5.56
1616325_at	protein coding	up	3.21
1621034_at	PCK1/PEPCK (phosphoenolpyruvate carboxykinase1)	up	3.97
1612546_at	Malate dehydrogenase protein coding	down	2.12
1610124_at	ribulose bisphosphate carboxylase small chain	down	6.66
1620673_at	fructose-bisphosphate aldolase	down	3.21
1610126_at	a spartate aminotransferase	up	24.56
1610868_s_at	protein coding	down	2.07
Porphyrin and chlorophyll metabolism			
1616605_at	Pheophorbide a oxygenase protein coding	up	2.62
Nitrogen metabolism			
1612389_at	glutamate dehydrogenase	up	6.41
1613113_at	phenylalanine ammonia-lyase	down	6.12
1610206_at	AT3G53260 P45724 phenylalanine ammonia-lyase 2 protein coding	down	2.46
1620767_at	glutamine synthetase	down	8.33
Starch and sucrose metabolism			
1612694_at	Galacturonosyltransferase 11 protein coding	down	2.44
1622282_at	protein coding	down	2.55
1609402_at	SUS3; UDP-glycosyltransferase/sucrose synthase/transferase, transferring glycosyl groups	up	2.93
Flavonoid biosynthesis			
1620675_at	dihydroflavonol reductase	down	33.58
1608212_at	leucoanthocyanidin reductase 2	down	2.99
1616191_s_at	ATC4H/C4H/CYP73A5(cinnamate-4-hydroxylase); 4-monooxygenase	down	6.47
Carotenoid biosynthesis			
1611359_at	Lycopene beta-cyclase/lycopene cyclase protein coding	down	2.60

In etiolated fruits, array analysis revealed relatively few genes with altered expression levels (Table 3). Concerning anthocyanin biosynthesis, the expression of the *BZI* gene, encoding UDP-glucose: flavonoid 3-O-glucosyltransferase (UFGT), was upregulated in albino fruits, with a 2.51-fold increase over wild-type levels. The *UFGT* gene is critical for anthocyanin biosynthesis, which affects grape coloration. Regarding porphyrin and chlorophyll metabolism in fruits, the *ATCAO* gene was downregulated, while the coproporphyrinogen-III oxidase gene, which is involved in chlorophyll catabolism, was upregulated.

Starch and sucrose metabolism have an important effect on grape quality and coloration. We found that the UDP-glucuronate 4-epimerase 6-like gene was upregulated in the etiolated grapevine, with an approximately 2.07-fold increase in expression over wild-type levels. Among the genes that were altered in etiolated fruits, secondary metabolic genes occupied a prominent position and were dominated by members involved in phenylpropanoid biosynthesis. Genes encoding glyceraldehyde-3-phosphate dehydrogenase c subunit and the hypothetical protein LOC100245746 were both upregulated in the etiolated grapevine.

**Table 3 Induced Genes in Etiolated Fruits**

Probe ID	Description	Regulation	Fold change
Anthocyanin biosynthesis			
1617171_s_at	UDP glucose:flavonoid 3-o-glucosyltransferase	up	2.51
Biosynthesis of phenylpropanoids			
1620724_at	hypothetical protein LOC100245746	up	2.26
Porphyrin and chlorophyll metabolism			
1620634_at	ATCAO	down	2.32
1610613_at	coproporphyrinogen-III oxidase	up	2.06
Photosynthesis			
1608562_at	ferredoxin--NADP reductase, leaf isozyme	up	2.25
Starch and sucrose metabolism			
1616405_at	UDP-glucuronate 4-epimerase 6-like	up	2.07
Biosynthesis of plant hormones			
1615814_at	Glyceraldehyde-3-phosphate dehydrogenase c subunit	up	2.11
1611487_at	hypothetical protein LOC100242104	up	3.96
1612190_at	hypothetical protein LOC100267750	down	2.09
1620724_at	hypothetical protein LOC100245746	up	2.26

### 3.5 Array Validation

To validate the microarray data, qRT-PCR was conducted on 14 genes selected randomly from each expression set. Positive correlations of transcription trends between microarray and qRT-PCR were obtained, except for 100266604 (1614598\_at), which showed weak downregulation on the array but displayed upregulation by qRT-PCR. The fold differences of several genes detected by qRT-PCR are displayed in Fig. 8. Generally, qRT-PCR and

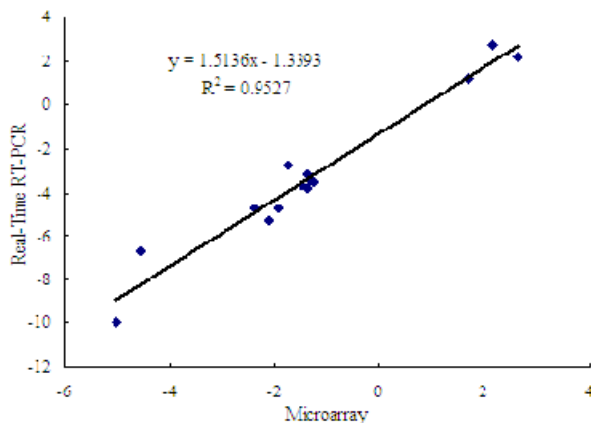
microarray data agreed quite well, indicating the robustness of the microarray data.

## 4. Discussion

### 4.1 Photosynthesis

Control plants performed better than etiolated grapevine plants during all phenological stages, not only due to the performance of the fruits, but also because of the lower photosynthetic rate of the etiolated grapevine. We further explored the differential photosynthetic capacities between the two

clones. Because leaves are photosynthetic organs that provide plants with carbohydrates essential for growth, and because leaf area is a significant contributor to productivity [11, 12], we chose leaves for microarray analysis in this investigation. In addition, Schmid et al. reported [13] that the expression levels of most genes in leaves were similar to those of the plant overall, establishing leaves as the prototypic organ system.



5-bisphosphate carboxylase-oxygenase (Rubisco) exhibited a decreased efficiency of photosynthesis at the biochemical level that was accompanied by an increased leaf area ratio, and decreased starch accumulation in the source leaves, allowing the transformant to make more efficient use of fixed carbon [19]. Steven J. (2000) [20] found that RuBisCo was deactivated in cotton and tobacco leaves in response to increased temperatures, high CO<sub>2</sub> levels, or low O<sub>2</sub> levels.

#### 4.3 Grape Coloration

Among the coloration genes with altered expression levels in the etiolated grapevine, genes involved in anthocyanin biosynthesis predominated (1 out of 1 gene). The *BZI* gene encoding UDP-glucose flavonoid 3-O-glucosyltransferase (UFGT) was found to have 2.51-fold upregulation compared with the control. The *UFGT* gene has been shown to be critical for anthocyanin biosynthesis in the grape berry. Using white grape cultivars and bud sports with red skin, Kobayashi S. (2001) [21] examined the expression of seven anthocyanin biosynthetic genes and found that the phenotypic change from white to red in the sports may have resulted from a etiolated grapevine in a regulatory gene controlling the expression of UFGT.

During the hard period of fruits, the etiolated grape fruits were bright yellow while the control fruits were the usual green color. We therefore analyzed changes in porphyrin and chlorophyll metabolism-related genes in etiolated fruits and leaves compared with the control and found that four out of 34 genes in fruits and five out of 34 genes in leaves were obviously altered in the etiolated grapevine. In leaves, approximately four genes were downregulated, all related to chlorophyll synthesis. The expression of only one gene that was altered in leaves was upregulated, namely, a gene encoding an iron-containing and ferredoxin-dependent monooxygenase, pheophorbide a oxygenase (PaO), which is composed of the oxygenase alpha subunits of a small subfamily of enzymes found in plants and

oxygenic cyanobacterial photosynthesizers including LLS1 (lethal leaf spot 1, also known as PaO) and ACD1 (accelerated cell death 1). PaO expression increases upon physical wounding of plant leaves and is thought to catalyze a key step in chlorophyll degradation. Tanaka R. (2003) produced transgenic *Arabidopsis* plants that expressed antisense RNA that inhibited the expression of PaO-encoding genes. The appearance of these antisense plants demonstrated that the inhibition of the gene involved in PaO activity leads to photooxidative destruction of the cell, negating the “stay-green” phenotype. In the current study, etiolated fruits exhibited upregulated expression of the gene encoding red chlorophyll catabolite reductase. The red chlorophyll catabolite reductase (RCC reductase) proteins RCC and pheophorbide (Pheide) a oxygenase (PaO) catalyze the key reaction of chlorophyll catabolism, porphyrin macrocycle cleavage of Pheide a to a primary fluorescent catabolite (pFCC).

Therefore, the downregulation of photosynthesis-related genes led to a lower photosynthetic rate (Pn), while the down-regulation of porphyrin and chlorophyll synthesis genes and the upregulation of degradation genes caused etiolated leaves and fruits to become light yellow. However, the enhanced capacity of carbon fixation in photosynthetic organisms and the more efficient import of chloroplast proteins may explain the survival of the etiolated branches.

#### References

- [1] M. R. Thomas, S. Matsumoto, P. Cain and N. S. Scott, Repetitive DNA of grapevine: Classes present and sequences suitable for cultivar identification, *Theor Appl Genet.* 86 (1993) 173-180.
- [2] M. A. Lodhi and B. I. Reisch, In situ hybridization in *Vitis vinifera* L., *Theor Appl Genet.* 90 (1995) 11-16.
- [3] N. Terrier, D. Glissant, J. Grimplet, F. Barrieu, P. Abbal, C. Couture, A. Ageorges, R. Atanassova, C. Léon, J. P. Renaudin, F. Dédaldéchamp, C. Romieu, S. Delrot and S. Hamdi, Isogene specific oligo arrays reveal multifaceted changes in gene expression during grape berry (*V. vinifera* L.) development, *Planta* 222 (2005) 832-847.

- [4] L. Fernandez, L. Torregrosa, N. Terrier, L. Sreekantan, J. Grimplet, C. Davies, R. M. Thomas, C. Romieu and A. Ageorges, Identification of genes associated with flesh morphogenesis during grapevine fruit development, *Plant Mol Biol* 123 (2006) 221-225.
- [5] Giorgia Albertazzi, Justyna Milc and Alessandra Caffagni, Gene expression in grapevine cultivars in response to Bois Noir phytoplasma infection, *Plant Sci* 176 (2009) 792-804.
- [6] H. K. Lichtenthaler, Chlorophyll and carotenoids: Pigments of photosynthetic biomembranes, *Method. Enzymol.* 148 (1987) 350-382.
- [7] M. A. Harris, J. Clark and A. Ireland, The Gene Ontology (GO) database and informatics resource, *Nucleic Acids Res* 32 (2004) 258-261.
- [8] Kenneth J. Livak and Thomas D. Schmittgen, Analysis of relative gene expression data using real-time quantitative PCR and the 2- $\Delta\Delta$ CT method, *Methods* 25 (2001) (4) 402-408.
- [9] O. Jaillon, J. M. Aury and B. Noel et al., The grapevine genome sequence suggests ancestral hexaploidization in major angiosperm phyla, *Nature* 449 (2007) 463-468.
- [10] M. Ashburner, C. A. Ball, J. A. Blake and D. Botstein, Gene Ontology: Tool for the unification of biology, *Nat Genet.* 25 (2000) (1) 25-29.
- [11] T. S. Barigah, B. Saugierb, M. Mousseaub, J. Guittetb and R. Ceulemansc, Photosynthesis, leaf area and productivity of 5 poplar clones during their establishment year, *Ann For Sci* 51 (1994) 613-625.
- [12] C. R. Ridge, T. M. Hinckley, R. F. Stettler, E. Van Volkenburgh, Leaf growth characteristics of fast-growing poplar hybrids *Populus trichocarpa*  $\times$  *P. deltoids*, *Tree Physiol.* 1 (1986) (2) 209-216.
- [13] M. Schmid, T. S. Davison, S. R. Henz, U. J. Pape, M. Demar, M. Vingron, B. Scholkopf, D. Weigel and J. U. Lohmann, A gene expression map of *Arabidopsis thaliana* development, *Nat Genet.* 37 (2005) (5) 501-506.
- [14] Anna Ihnatowicz, Paolo Pesaresi, Claudio Varotto, Erik Richly and Anja Schneider, Mutants for photosystem I subunit D of *Arabidopsis thaliana*: Effects on photosynthesis, photosystem I stability and expression of nuclear genes for chloroplast functions, *Plant J.* 37 (2004) (6) 839-852.
- [15] Yoshiharu Y. Yamamoto, Masayuki Nakamura and Yukiko Kondo, Early Light-Response of *psaD*, *psaE* and *psaH* Gene Families of Photosystem I in *Nicotiana sylvestris*: PSI-D has an Isoform of Very Quick, *Plant Cell Physiol.* 36 (1995) (4) 727-734.
- [16] Yoshiharu Yamamoto, Hideo Tsuji and Junichi Obokata, Structure and expression of a nuclear gene for the PSI-D subunit of photosystem I in *Nicotiana sylvestris*, *Plant Mol Bio.* 22 (1993) (6) 985-994.
- [17] Ying Zhou, Hongmei Cai, Jinghua Xiao, Xianghua Li, Qifa Zhang and Xingming Lian, Over-expression of aspartate aminotransferase genes in rice resulted in altered nitrogen metabolism and increased amino acid content in seeds, *Theor Appl Genet.* 118 (2009) (7) 1381-1390.
- [18] Susan E. Wilkie, Jennifer M. Roper, Alison G. Smith and Martin J. Warrant, Isolation, characterization and expression of a cDNA clone encoding plastid aspartate aminotransferase from *Arabidopsis thaliana*, *Plant Mol Bio.* 27 (1995) (6) 1227-1233.
- [19] R. Tanaka, M. Hirashima and A. Tanaka, Mechanisms for high light acclimation studied with transgenic *Arabidopsis* plants overexpressing chlorophyllide a oxygenase, *Plant Cell Physiol.* 44 (2003) 142.
- [20] J. Steven, Crafts-Brandner and Michael E. Salvucci, Rubisco activase constrains the photosynthetic potential of leaves at high temperature and CO<sub>2</sub>, *PNAS.* 97 (2000) (24): 13430-13435.
- [21] M. Kobayashi, Ishimaru and C. K. Ding, Comparison of UDP-glucose: Flavonoid 3-O-glucosyltransferase (UFGT) gene sequences between white grapes (*Vitis vinifera*) and their sports with red skin, *Plant Sci.* 160 (2001) (3) 543-550.